

STUDY OF WIM SENSOR ELECTRO-MECHANICAL BEHAVIOR: A MODEL IN THE FREQUENCY DOMAIN



G.G. OTTO
UFSCs
Brazil



J.M. SIMONIN
IFSTTAR
France



J.M. PIAU
IFSTTAR
France



L. MOMM
UFSC
Brazil



A.M. VALENTE
UFSC
Brazil

Abstract

This article aims to propose a model of WIM piezoelectric sensor to help better understand the mechanical and electrical properties when installed on the road. The model consists in represent the sensor electric response using a tire load and the pavement deflection (response to the load effect), together representing the electromechanical behavior. Tests in laboratory and in the fatigue carousel test track are used to access the coefficients of the model. In laboratory, two types of test are design, one pure punching and another three-point bending test. The pure punching allows accessing the coefficient that correlates the effect of the force only. The three-point bending test allows accessing both coefficients. In the fatigue carousel, the three types of sensors are tested with FWD and with a metallic plate over the sensors. The results presented in this article confirms some of the sensor electric characteristics, but also show new characteristics related to sensor position of the load and pavement response.

Keywords: Piezoelectric sensor, WIM sensors, WIM sensor electric mechanic model, Weigh-in-Motion, WIM, Pavement and sensor interaction, Pavement mechanic characteristics.

Resumo

Este artigo tem como objetivo propor um modelo de sensor piezoelétrico WIM que permita melhorar a compreensão das propriedades mecânicas e elétricas quando instalados em rodovias. O modelo consiste em representar a resposta elétrica do sensor utilizando a carga de um pneu e a deflexão do pavimento. São utilizados testes em laboratório e na pista de testes do carrossel de fadiga para avaliar os coeficientes definidos pelo modelo. Em laboratório, dois tipos de testes são organizados, uma compressão direta e outra flexão-3-pontos. O teste de compressão direta permite avaliar diretamente o coeficiente que correlaciona o efeito isolado da carga sobre o sensor. O teste de flexão-3-pontos permite avaliar ambos os coeficientes. No carrossel de fadiga, todos os tipos de sensores são testados com o equipamento FWD e com uma placa metálica sobre os sensores. Os resultados apresentados neste artigo confirmam algumas características elétricas dos sensores, mas mostram também novas características relacionadas a posição da carga e da resposta do pavimento.

Palavra-chave: Sensores piezoelétricos, sensores WIM, modelo eletromecânico de sensores WIM, Pesagem em movimento, WIM, Resposta sensor e pavimento, Características mecânicas de pavimentos.

1. Introduction

The weigh-in-motion (WIM) systems can have many applications, such as traffic counting, vehicle classification, axle load measurements, all kind of applications on traffic monitoring. WIM systems have been used for a while to data collection and pre-selection of over loaded trucks (COST-323, 1998). Today pavement managers have a demand for more accuracy. Thus, many research institutes are studying ways to improve data quality and system accuracy.

Many aspects can influence the WIM system accuracy, the quality of the sensors, the pavement behavior, temperature and the traffic and vehicle as they pass by the sensors zone (DNIT-UFSC, 2009a). In addition, the performance of any WIM system is dependent on road conditions, road geometry, and vehicle condition (DNIT-UFSC, 2009b). This paper specifically deals with the interaction between WIM sensors and the pavement response. Scheuter (1998) have study many factors affecting the WIM system accuracy. He established typical sensor accuracy and dependence on external factors such as intrinsic sensor error, longitudinal tilt, changing of position, pavement evenness, vehicle suspension, tire and speed.

To address these aspects, we first propose a numerical model that represents the WIM sensor electric response under the influence of an axle load and pavement deflection. Then we perform different laboratory tests to characterize the sensor behavior under different conditions of support and loading. The results are used to identify the model parameters.

Tests in the fatigue carousel at IFSTTAR/Nantes with different ways of stimulation helped to studying the in-situ behavior in more realistic traffic condition. In parallel, the sensor model was implemented in to pavement design code to simulate sensor response taking into account the pavement deflection. Finally, we compare the theoretical results with the experimental ones.

This project is part of a cooperation between two institutions the French Institute of Science and Technology for Transport, Development and Networks (IFSTTAR) and the Federal University of Santa Catarina (UFSC), by Transportation and Logistics Laboratory (LabTrans), in cooperation with the National Department of Transport Infrastructure (DNIT) of Brazil. The main goal for both countries is to use the WIM technologies to perform direct enforcement of overloaded vehicle on the main traffic stream. The development of this project was funded by the General Direction of Infrastructures, Transport and Sea (DGITM) within the frame of a research projects coordinated by IFSTTAR.

2. WIM sensors

The strip sensor with quartz technology are deliver as bars. The external part is an aluminum profile and inside there are several pastilles of quartz distributed separately from each other but connected by conductive element to the output. The internal form of the sensor allow only vertical effort to stimulate the internal pastilles. The ceramics sensor is generally made of powder ceramic compress inside of a metallic profile (some types are design as a tube). In the core there is a central core made of copper, which is connect to the output. The polymer strip sensor is composed by a polymeric film spiral-wrapped PolyVinylidene Fluoride – PVDF inside of a copper flat tube. The optical sensor is design with a fiber optic inside of a dense foam. There are two known principles of measurement, one evaluates the decrease of optical transmittance. An optic-electronic interface detects the changes in the optical signal and

transforms them into signals for traffic data processing. The strain gauge strip sensor uses strain gauges inside of a metallic profile, it transforms strain measurement into equivalent axle weight.

3. Electro mechanic general model proposition

By definition here, the WIM sensor is a piezoelectric bar. Supposing that the electrical charge (or tension on exit of the charge amplifier) produced all along the sensor is linear dependent of the force $f^*(s)$ apply on the surface (the load to measured) and the curvature $C^*(s)$ (related to the deflection of the pavement and of the beam). Following equation is produced.

$$Q^* = \int_0^l p^*(s) f^*(s) ds + \int_0^l r^*(s) C^*(s) ds \quad (1)$$

where: Q^* is the complex amplitude of the output electrical charge measured, $f^*(s)$ and $C^*(s)$ are the complex amplitudes of the force the curvature along the sensor. $p^*(s)$ and $r^*(s)$ are two complex functions to be determined, which are eventually function of the frequency ω and the temperature θ .

In the expression (1), we consider electric charge produced as linear dependent on the all forces encountering the sensor contact with the pavement and the sensor curvature. Consequently, one formulation based on support reactions will have the same equivalent effect.

In laboratory test we use a punctual force applied at different points of the sensor surface, instead of distribute pressures. In the case of a one punctual force F^* over the sensor applied at abscissa s^0 , we can write:

$$f^*(s) = F^* \delta(s - s^0) \quad (2)$$

$$Q^*(s) = p^*(s^0) F^* + \int_0^l r^*(s) C^*(s) ds \quad (3)$$

where $\delta(s - s^0)$ is Dirac distribution.

If we suppose r^* independent of s , from the relationship between deflection Y^* and curvature, $C^*(s) = \frac{\partial^2 Y^*}{\partial s^2}$, we can deduce the expression (4).

$$Q^* = p^*(s^0) F^* + r^* \left(\frac{\partial Y^*}{\partial s}(l) - \frac{\partial Y^*}{\partial s}(0) \right) \quad (4)$$

The term $\Delta P^* = \frac{\partial Y^*}{\partial s}(l) - \frac{\partial Y^*}{\partial s}(0)$ represents the complex amplitude of the difference between slopes (algebraic) of the bar between its extremities.

To identify the functions p^* and r^* in laboratory, two testing modes can be used:

- One by pure punching with the sensor-bar put over an infinitely rigid support. In this case, the curvature C^* is equal to zero and the sensor electrical response depends uniquely of the force and the coefficient $p^*(s^0)$, which can then be directly measured:

$$Q^* = p^*(s^0) F^* \quad (5)$$

- The other one by the three-point bending test, which make possible to identify both p^* (s^0) and r^* , considering different support spans. Assuming a linear mechanical behavior of the bar, we can determine the geometrical factor φ_i^* , for each span ($i = 1, 2, \dots$) and given frequency, so that:

$$\frac{\partial Y_i^*}{\partial s}(l) - \frac{\partial Y_i^*}{\partial s}(0) = \varphi_i^* F^* \quad (6)$$

Applying into the equation (4) we have the equation (8).

$$Q_i^* = (p^*(s^0) + r^* \varphi_i^*) F_i^* \quad (7)$$

For $i > 2$, this system can be solved by the least square method. In the case of two equations only, we get:

$$p^* = \frac{1}{\varphi_1^* - \varphi_2^*} \left(-q_1^* \frac{Q_2^*}{F_2^*} + q_2^* \frac{Q_1^*}{F_1^*} \right) \quad (8)$$

$$r^* = \frac{1}{\varphi_2^* - \varphi_1^*} \left(\frac{Q_2^*}{F_2^*} - \frac{Q_1^*}{F_1^*} \right) \quad (9)$$

- One in pavement when the wheel is approaching the sensor without touching it, or making the wheels rolling over a little metal plate covering the sensor without contact with its surface. In these cases, the force F^* is equal to zero. The sensor electrical response depends uniquely of the curvature and the coefficient r^* .

$$Q^* = \int_0^l r^* C^*(s) ds \quad (10)$$

4. Laboratory tests

The piezoelectric quartz and ceramic sensors technologies are the only two tested in laboratory. The first one is a 1.75m quartz base sensor, which is rigid enough to be tested without any mounting support. The second is a 3.6m ceramic base sensor, which is not rigid enough and a mounting adaptation is needed.

Both p^* and r^* are determined in laboratory. Using a hydraulic press mounted in a metallic structure support. The sensor stays positioned under the contact piston. The press has a 7kN capacity, which can displace in the vertical plane. The maximum displacement speed is 2m/s and the maximum frequency of 1kHz. The contact of the piston is a spherical joint type, to ensure that the force is perpendicular to the sensor surface every time. In the punching test, the sensor stays over an unreformed metallic bar (see (A) in Figure 1). In the three-point bending test the sensor stays over two cylindrical supports and the piston stays at central position, with respects to the two supports (see (B) in Figure 1).



Figure 1 – In (A) details of the punching test, in (B) the details of the three-point bending test

4.1 Punching test

During the punching test with the Quartz sensor, a sinusoidal force is applied on the sensor (5, 10 and 20Hz) with amplitude of 3kN. A pre-charge of 0,5kN maintains the contact between the piston and the sensor surface. Temperature is constant and around of 25°C. The force signal, sensor electrical response, piston displacement and external displacement sensor are recorded. The punching test is done in each sensor during the manufacturing process. The results here can be compared to the sensor calibration sensitivity from the manufacturer.

69 measurements total are performed at each 2.5cm over the sensor surface. Variation of sensitivity along the sensor is identify. The sensor electrical response confirm that the sensor is constitutes by small pastilles space every 5 cm. For a distributed force, like a pneumatic, several pastilles are stimulate reducing dispersion of a single point sollicitation. Figure 2 show the moving average for different frequencies (5, 10 and 20Hz), also show that the sensor response has a frequency dependence. Over all frequencies, the maximum sensitivity was 1.75 and response dispersion over all measurements of 1.7%. The sensitivity variation along the sensor length means that for a high accuracy WIM system, the tire position must be taken into account.

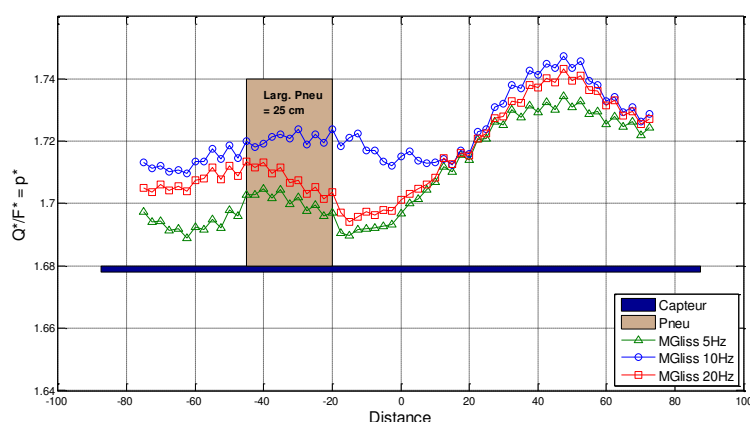


Figure 2 – Moving average of the electrical response at different positions for different frequencies

4.2 Three-point bending test

In the three-point bending test, the piston stays in the center of the two supports. A sinusoidal force is applied in several frequencies are tested between 0.5 and 25Hz. Temperature

remained at 25°C. Three supports span was chosen ($E1 = 77$, $E2 = 57$ cm and $E3 = 57$ cm, displacing the sensor in 15cm). Sensor was positioned in normal position (Face A) and inverse (Face B). Figure 3 shows the values of p^* (A) and r^* (B) calculated for each test frequency. The difference on the sensor response, between the normal position and inverse, is represented by the difference of sign on the values of r^* .

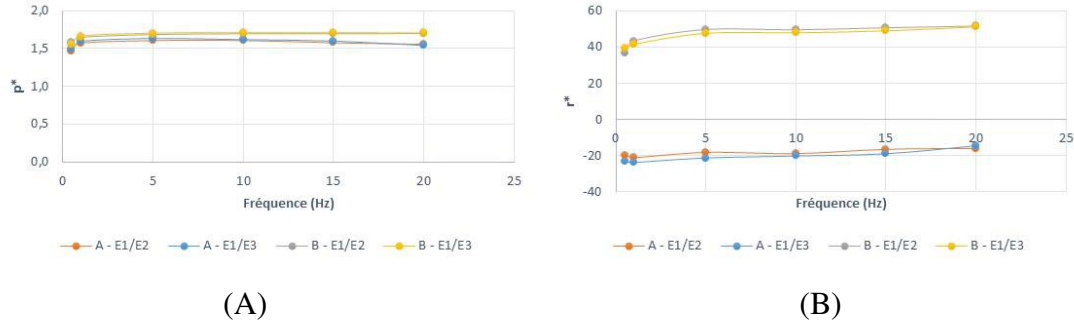


Figure 3 – In (A) the values for p^* and in (B) values of r^* , calculated for the modalities E1 and E2 (Face A and B) and E1 and E3 (Face A and B).

To determine how important p^* and r^* are to the sensor electrical response, we assume a real situation. Under a load of 65kN, the deflection of a typical structure of the national road network in France generally is below of 0.40mm with a radius of curvature at the top of the order of 2000m. In these conditions, the curvature of the pavement surface is 1/2000 under the load and it gets smaller far from the center of solicitation. Supposing the curvature of 1/2000m constant in the expression (3), conducts to overestimate the part related to the curvature. The sensor in normal position (Face A) have $p^* = 1.6$ and $r^* = -18.1$. The sensor electrical response can be assumed.

$$Q^* = 1.6 \times F^* - \int_0^l 18.1 \times C^*(s) ds \quad (11)$$

The part that represents the curvature $C^*(s)$ along in the sensor length of 1.75m is equal to: $18.1 \times \int_0^l C^*(s) ds = 18.1 \times \int_0^{1.75} \frac{1}{2000} ds = 18.1 \times 0.000875 = 0.016$.

The part that represents the force F^* for 65kN is equal to: $1.6 \times 65 = 103.5$.

The total electrical response is: $Q^* = 103.5 - 0.016 = 103.516$.

The response is 99.98% related to the superficial stress and 0.02% to the curvature. In the case of inverse curvature, the sensor response still would be below of 0.02%. This represents that the response part related to the sensor curvature can be neglected.

5. In-situ tests

The fatigue carousel test track is a circular track. It has a circumference of 120m at the radius of 19m. The in-situ tests main proposal is to stimulate the sensors in two different conditions: one pure bending without the load direct over the sensor, and another, conjugating the bending and the load action over the sensor. The metal plate and FDW equipment (see Figure 4 (A) and (B) respectively), placed over the WIM sensors, can reproduce these two conditions.



Figure 4 – The image (A) shows the metal plate covering one sensor, the plate details and alignment with sensor, in the image (B) show the FWD trailer positions relatively to the sensor

5.1 Quartz sensor

Figure 5 compare the two signals from the acquisition of the quartz sensor. The graphic above presents the two signals, the response of the sensor in normal condition (without the metal plate) and in blue, the sensor response covered with the plate (deflection only). The weak signal intensity, the graphic bellow presents a zoom at the ordinates axle. The relation between maximal amplitudes is less than 0.3%. The deflection sensitivity of this sensor on deflection is neglected compared with the sensitivity founded to test punching solicitation.

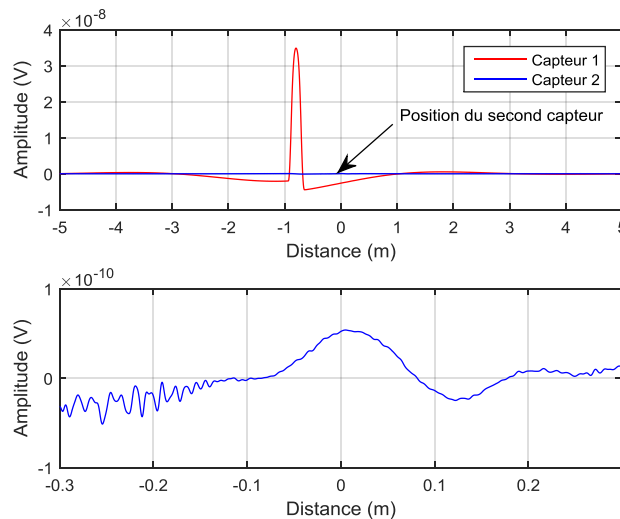


Figure 5 – Comparison of the piezoelectric quartz sensor response, in blue the presence of the plate (flexion only) and in red the sensor in normal condition (flexion and punching)

Figure 6 shows the comparison of the same sensor responding to the solicitation of the equipment. In red is the FWD plate over the sensor, in blue the plate beside the sensor top surface. Comparing the two sensors maximal amplitudes is less than 0.2%, showing once more that the sensor sensitivity to deflection only can be neglected.

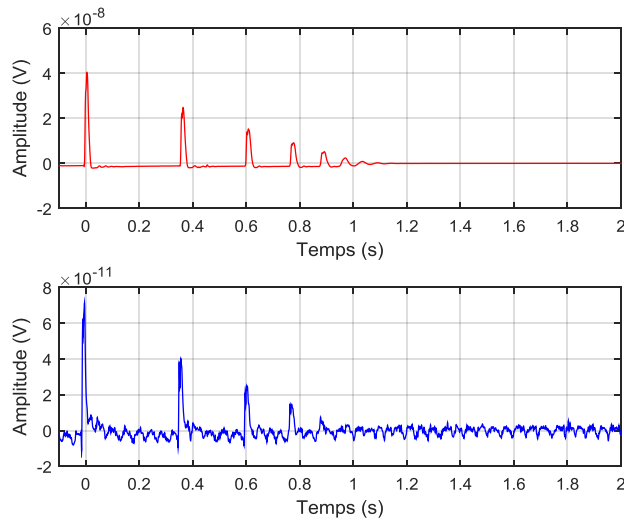


Figure 6 – Comparison between sensor response in the FWD test, above is the sensor response with the FWD plate over the sensor, below, in blue, is the sensor response with the FWD plate just beside the sensor surface

5.2 Ceramic sensor

Figure 7 present the same signal comparison in the test with the metal plate covering the piezo ceramic sensor and the normal situation. In this situation, the signal scale in the ordinates is about 3.33. The signal observed in the presence of the metal plate cannot be neglected. It represents up to 25% of the measure level. The pavement stiffness, consequently its deflection, will generate an influence over the measure level for this lows speed test (about 1 rpm).

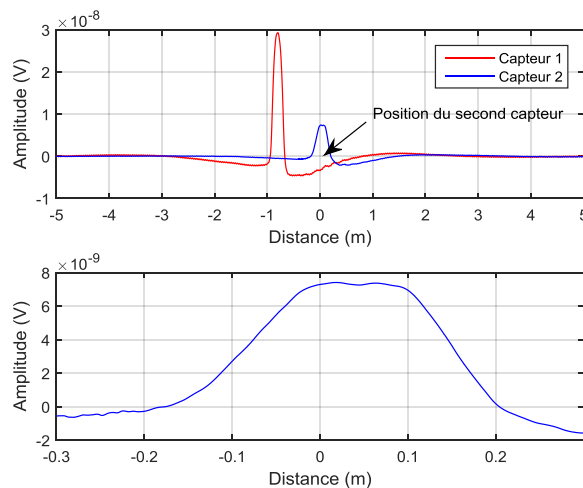


Figure 7 – Comparison of the piezoelectric ceramic sensor response, in blue the presence of the plate (flexion only) and in red the sensor in normal condition (flexion and punching)

The two signal acquired of the same sensor (ceramic technology), presented in Figure 8 above, the first FDW impact and the subsequent chocks. The graphic below corresponds to the signal when the FWD plate beside the sensor top surface. The scale of ordinate axle is

adapted in each case. In the second case, it corresponds an amplification factor of 15. The maximal amplitude relation, difference maximal value and the minimal, is approximately 10%. The pavement deflection sensitivity can be not neglected and is estimated less than 10%. No doubt that this sensitivity is superior, because de maximal deflection measured at 30 cm away from the load represent approximately 65% of the maximal deflection under the load.

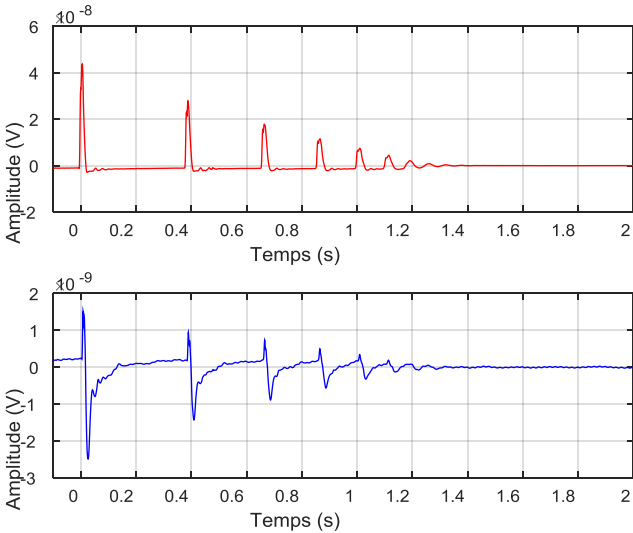


Figure 8 – Comparison between sensor response in the FWD test, above is the sensor response with the FWD plate over the sensor, below, in blue, is the sensor response with the FWD plate just beside the sensor surface

6. Conclusions

The piezo quartz sensor, during the punching test, show that the sensors sensitivity varies according to the load position across the sensor surface. This sensitivity variation is estimated as 1.75%, which is close to the characteristics provide by the manufacturer (< 3%). In other words, knowing the position of the tire associated to the sensor calibration at this point is the way to reduce some of the uncertainty. The results obtained shows for the punctual charge a variation of sensitivity along the sensor approximately of 2.91%. The punctual test allows reaching directly the p^* value, the mean value of the sensitivity of p^* is 1.72pC/N.

The same sensor in the three-point bending shows independence of the mechanical behavior flowing the sensor orientation (normal or inverted). Differently, the electrical response is dependent of the sensor orientation, which means to conjugate the precedent conclusion where the curvature is negative or positive he sensor response may be different due to deflexion effects. The test puts in evidence the electrical response sensitive to low frequency sollicitation, but is constant by 5 Hz. In real situation, the vehicle speed is much higher to this frequency. The estimated sensitivity p^* , at normal position (face A), is about 1.60pC/N. Different from the sensitivity coefficient deduced by the punching test, by 7%, resulted because of the different configuration between the two types of test.

The in-situ test confirms the sensor behavior observed in laboratory tests, both technology. The results indicate that the sensitivity of the quartz due flection can be neglected if compared with the punching effect in normal condition of measurement.

The ceramic sensor response recorded shows the strong sensitivity to deflection, which represents about 10 up to 30% of the maximal level of measurements. The signal processing should take into account this strong influence. To improve the ceramic sensor signal, a complex modeling of the pavement and sensor it is necessary with rigorous laboratory characteristics of the electro mechanic parameters.

7. References

- DNIT_UFSC (2009a). “Relatório de testes em campo”, in *Project Report.: Identificação de Sistemas de Pesagem em Movimento*, Convênio TT 102/2007, LabTrans, UFSC, DNIT, Minister of Transportation, Brasília, Brazil.
- DNIT_UFSC (2009b). “Relatório de avaliação dos resultados”, in *Project Report.: Identificação de Sistemas de Pesagem em Movimento*, Convênio TT 102/2007. UFSC, DNIT, Minister of Transportation, Brasília, Brazil.
- Scheuter, F (1998). “Evaluation of Factors Affecting WIM System Accuracy”. *Pre-proceeding of 2nd European Conference on Weigh-in-Motion of Royal Vehicles*, Lisbon 14-16 September. Luxemburg: European Commission, 371-380.
- COST 323 (1999). “Weigh in motion of road vehicle”. *EUCO-COST/323/8/99*, LCPC, Paris, August, 66 pp.